

Study of Two BeppoSAX Observations of GX 340+0

R. Iaria¹*, G. Lavagetto¹, T. Di Salvo¹, A. D’Ai¹, L. Burderi², L. Stella³ and N. R. Robba¹

¹ Dipartimento di Scienze Fisiche ed Astronomiche, Università di Palermo, via Archirafi 36, 90123 Palermo, Italia

² Università degli Studi di Cagliari, Dipartimento di Fisica, SP Monserrato-Sestu, KM 0.7, 09042 Monserrato, Italia

³ Osservatorio Astronomico di Roma, Via Frascati 33, 00040 Monteporzio Catone (Roma), Italia

Abstract We present the results of two BeppoSAX broad band (0.1–200 keV) observations of the Z-source GX 340+0 comparing our results to those of a previous observation of the source. From the color–color diagram we selected three zones and extracted the source energy spectrum from each zone. We find that the model, composed by a blackbody plus a Comptonized component, absorbed by an equivalent hydrogen column of $\sim 6 \times 10^{22} \text{ cm}^{-2}$, well fits the spectra in the energy range below 30 keV. At higher energies a power law component with photon index of 2.5 is observed. The associated flux decreases going from the horizontal branch to the flaring branch of the Z-track.

Key words: stars: individual (GX 340+0) — X-rays: binaries — X-rays: general

1 INTRODUCTION

GX 340+0 is a Z source not well known. It was detected as a Galactic X-ray source by Friedman, Byram & Chubb (1967) and its position was determined by Rappaport et al. (1971) with a precision of $1'$. The system was identified as a neutron star (NS) binary system by Margon et al. (1971) on the basis of data carried out from an Aerobee rocket. Ariel V data of GX 340+0 showed a positive correlation of spectral hardness with intensity (Ponman, 1982), while the CD and the hardness-intensity diagram of the source, obtained from EXOSAT data (van Paradijs et al., 1988), indicated that GX 340+0 has a positive correlation between the hardness ratio (HR), defined as $[6\text{--}20 \text{ keV}]/[3\text{--}6 \text{ keV}]$, and the intensity in the 1–20 keV energy range when $\text{HR} < 0.4$, while at $\text{HR} \simeq 0.4$ the intensity reduced with no changes in HR (see figs. 3c and 4c in Schulz et al., 1989). The change of correlation between the intensity and HR happened roughly at the highest hardness values indicating a hard apex. Schulz et al. (1989) noted that, in analogy to Cyg X–2, the data formed a horizontal branch (HB)–normal branch (NB) pattern. Taking also in account that Garcia (1987) found indications of a third spectral branch at the soft end of the NB in an analysis of HEAO 2 MPC data, Schulz et al. (1989) suggested that GX 340+0 showed a Z-shaped spectral variation pattern. The correlated power spectral and X-ray spectral behavior of the source, described by van Paradijs et al. (1988), allowed to classify it as a Z source (Hasinger & Van der Klis, 1989). A unique spectral analysis of the source was carried out by Schulz et al. (1993) using EXOSAT data in the 2–12 keV energy range. The spectrum was fitted by a blackbody, with a temperature of 0.8 keV, plus a Comptonized component, with an electron temperature ranging between 4 and 6 keV, absorbed by an equivalent hydrogen column density of $\sim 4 - 5 \times 10^{22} \text{ cm}^{-2}$. However the residuals (see fig. 4 in Schulz et al., 1993) seemed to indicate that the spectrum of GX 340+0 is more complex. Penninx et al. (1993) identified the radio counterpart of GX 340+0 with an accuracy of $\sim 3''$. Using the coordinates of the radio counterpart Miller et al. (1993) detected an infrared source having a magnitude of 17.3 ± 0.5 mag in the K band as possible infrared counterpart of

* E-mail: iaria@fisica.unipa.it

GX 340+0. The radio measurements allowed to estimate the distance to the source of 11 ± 3 kpc (Fender & Hendry, 2000)

Recently Lavagetto et al. (2004) studied the 0.1–200 keV energy spectrum of GX 340+0 spectrum using BeppoSAX data carried out between 2001 August 9 and 10 (thereafter Observation 3). They obtained an equivalent hydrogen column associated to the interstellar matter of $N_{\text{H}} \sim 6.2 \times 10^{22} \text{ cm}^{-2}$ finding that the spectrum below 30 keV could be fitted by a blackbody component (with a temperature of $kT_{\text{BB}} \sim 0.51$ keV) plus a Comptonized component (with a seed-photon temperature of $kT_0 \sim 0.93$ keV and an electron temperature of $kT_e \sim 3$ keV). At higher energies a power-law component with a photon index of 2.5 was present, finally a Gaussian emission line at 6.75 keV, associated to Fe XXV, was observed.

In this paper we report the results of a spectral study of GX 340+0 in the 0.1–200 keV energy range based on BeppoSAX data from two observations carried out between 2000 August 16 and 20, and 2001 March 9 and 11, thereafter called Observation 1 and Observation 2, respectively.

2 OBSERVATIONS

During the two observations the four co-aligned Narrow Field Instruments (NFIs; Boella et al., 1997) on board BeppoSAX were used. The exposure times of each instrument for each observation were reported in Table 1.

Table 1 Some details of the three BeppoSAX observations of GX 340+0. We report in the second and third columns the start and stop times of the observations, from the fourth to the seventh columns the exposure times of each instrument for each observation.

Observation	Start Time (UT)	Stop Time (UT)	LECS ks	MECS ks	HPGSPC ks	PDS ks
1	2000-08-16:05:50:34.0	2000-08-20:14:21:16.0	52.5	123	138	60
2	2001-03-09:19:27:20.5	2001-03-11:11:13:47.0	18.5	54.5	56	28

In Figure 1 (left panel) we showed the 300 s binned lightcurve of GX 340+0 in the 1–10 keV energy band during the Observation 1. The count rate was between 80 counts s^{-1} and 110 counts s^{-1} showing clearly two states of the source: a low state, when the count rate was 80 counts s^{-1} and a high state, when the count rate was 100–110 counts s^{-1} . In Figure 1 (right panel) we showed the 300 s binned lightcurve of GX 340+0 in the 1–10 keV energy band during the Observation 2. The count rate was between 80 counts s^{-1} and 120 counts s^{-1} , differently from the Observation 1 the count rate was highly variable during the whole observation.

We extracted the CD of GX 340+0 and showed it in Fig. 2 (left panel). The hard color (HC) was the ratio between the count rate in the 7–10 keV energy band to that in the 3–7 keV energy band and the soft color (SC) was the ratio between the count rate in the 3–7 keV energy band to the count rate in the 1–3 keV energy band. All of the three observations were plotted using a bin time of 8 ks. In the plot we indicated the observations 1, 2 and 3 with red, green and blue data, respectively. We noted that, during the first and the second observation, the SC and the HC were positive correlated, with SC ranging between 4.6 and 5.8 and HC ranging between 0.10 and 0.17, while during the third observation the position of the source was localized to $\text{SC} \sim 5.5$ and HC ranging between 0.18 and 0.21. To well identify a possible correlation between the intensity and the HR of the source we extracted the hardness-intensity diagram (HID), showed in Fig. 2 (Right Panel). The HR was the SC above defined, respectively, and the count rate was in the 1–10 keV energy band (MECS data).

The HID indicated a positive correlation between HR and intensity during observation 1 and 2, while, during observation 3, the HR defined as the ratio $[3 - 7 \text{ keV}]/[1 - 3 \text{ keV}]$ was constant to 5.5 with an intensity ranging between 60 and 70 counts s^{-1} . The CD and HID (Fig. 2) seemed to suggest that GX 340+0 was probably in the HB, during Observation 3, and in the NB down to the soft apex of the Z track, during Observation 1 and 2. Because of the different spectral behaviour of the source along the Z track we selected three zones on the CD (see Fig. 2) and extracted the corresponding energy spectra from each zone. We called the three zones A, B and C, corresponding to the lower NB, upper NB and HB, respectively. Note that Observation 3, analyzed in Lavagetto et al. (2004), entirely fell in the zone C of the CD. In Table 2

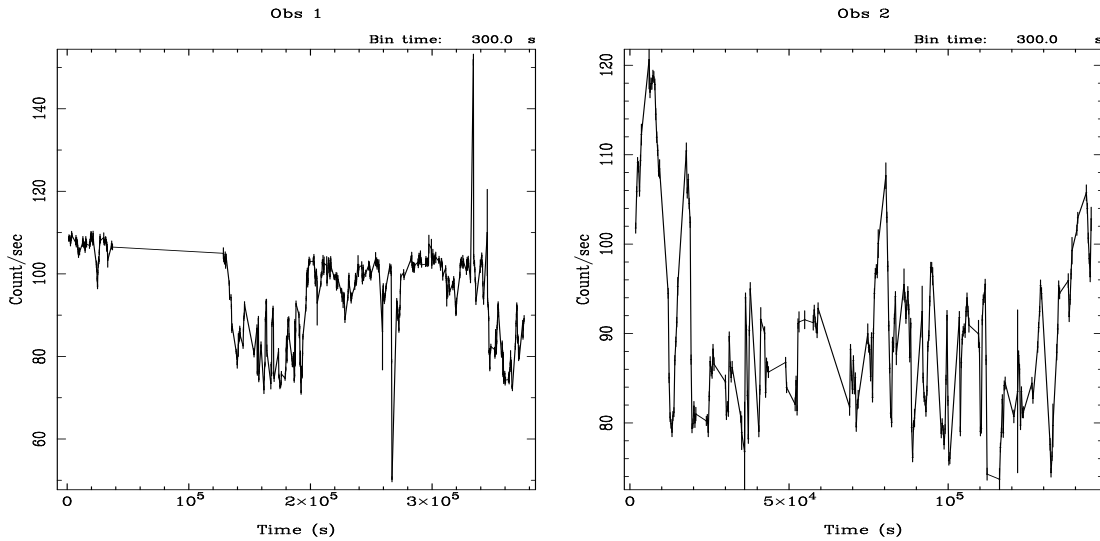


Fig. 1 GX 340+0 lightcurves in the energy band 1–10 keV (MECS data) corresponding to the Observation 1 (Left Panel) and Observation 2 (Right Panel). For sake of clarity we interpolated the events. The bin time is 300 s.

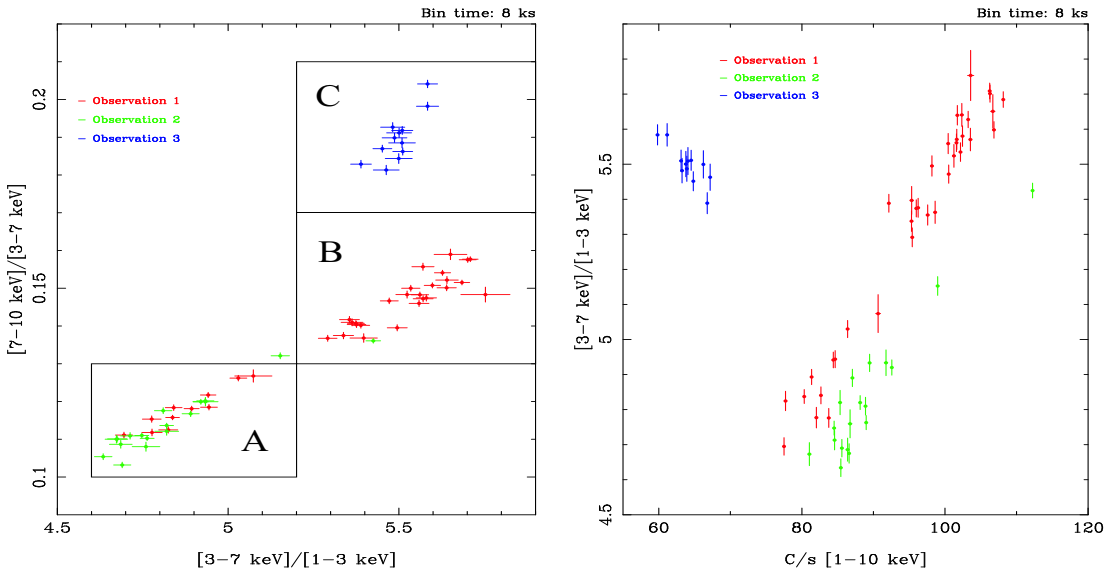


Fig. 2 Color-color diagram (left panel) and Hardness-Intensity diagram (right panel) of GX 340+0. The hard color is the hardness ratio $[7-10 \text{ keV}]/[3-7 \text{ keV}]$, the soft color is the hardness ratio $[3-7 \text{ keV}]/[1-3 \text{ keV}]$, and the intensity of the HID is the count rate in the 1–10 keV energy range. The bin time is 8 ks. The boxes in the CD indicate the three selected zones from which we extracted the corresponding energy spectra. Observation 3 was analyzed by Lavagetto et al. (2004)

we reported the intervals of SC and HC which identified the three selected zones; the exposure times of the LECS, MECS, HPGSPC and PDS for each of the three intervals were also reported.

3 ANALYSIS AND DISCUSSION

The PHA spectra of the LECS, MECS, HPGSPC, and PDS were rebinned in order to have at least 25 counts/energy channel and to oversample the instrumental energy resolution by approximately the same

Table 2 Some details of the zones in which the color-color diagram was divided. In columns 2 and 3 we report the intervals of Soft Color (SC) and Hard Color (HC) which identify the three selected zones in the color-color diagram (see Fig. 2). In the other columns the corresponding exposure times, in ks, of the LECS, MECS, HPGSPC and PDS, respectively.

Zone	SC interval	HC interval	LECS ks	MECS ks	HPGSPC ks	PDS ks
A	4.6–5.2	0.100–0.130	33	88	93	45
B	5.2–5.9	0.130–0.160	37	86	98	41
C	5.2–5.9	0.170–0.210	19	47	46	23

Table 3 Results of the spectral fit in the 0.12–200 keV energy band of Spectra A, and B with a model composed of a blackbody plus a Comptonized component (Comptt in XSPEC) and a power-law component, both absorbed by neutral matter. Uncertainties are at 90% confidence level for a single parameter, upper limits are at 95% confidence level. kT_{BB} and N_{BB} are, respectively, the blackbody temperature and normalization in units of L_{39}/D_{10}^2 , where L_{39} is the luminosity in units of 10^{39} erg s $^{-1}$ and D_{10} is the distance in units of 10 kpc. kT_0 is the temperature of the seed photons for the Comptonization, kT_e is the electron temperature, τ is the optical depth of the scattering cloud using a spherical geometry, N_{comptt} is the normalization of the Comptt model in XSPEC v.11.3.0 units. N_{po} is the normalization of the power-law component in units of photons keV $^{-1}$ cm $^{-2}$ at 1 keV. The fluxes are in units of 10^{-8} erg s $^{-1}$ cm $^{-2}$. L_{tot} is the unabsorbed luminosity in the 0.12–200 keV energy range. $E_{\text{Fe XXV}}$, $\sigma_{\text{Fe XXV}}$, $I_{\text{Fe XXV}}$ and $\text{EQW}_{\text{Fe XXV}}$ are the centroid, the width, the intensity and the equivalent width of the absorption line. $I_{\text{Fe XXV}}$ is in units of photons cm $^{-2}$ s $^{-1}$

Parameters	A	B	C
Continuum+Line	NB/FB	NB	HB
N_{H} ($\times 10^{22}$ cm $^{-2}$)	6.28 ± 0.13	6.50 ± 0.15	$6.16^{+0.26}_{-0.30}$
kT_{BB} (keV)	$0.597^{+0.036}_{-0.032}$	0.640 ± 0.028	$0.503^{+0.036}_{-0.017}$
N_{BB} ($\times 10^{-2}$)	7.83 ± 0.28	6.80 ± 0.43	4.10 ± 0.60
Flux _{BB}	0.66	0.57	0.34
R_{BB} (km)	66.0 ± 7.0	70 ± 10	78 ± 18
kT_0 (keV)	$1.206^{+0.023}_{-0.019}$	$1.109^{+0.037}_{-0.032}$	0.930 ± 0.060
kT_e (keV)	$5.7^{+5.4}_{-1.3}$	$2.996^{+0.060}_{-0.057}$	3.000 ± 0.030
τ_{comptt}	2.9 ± 1.3	8.90 ± 0.27	12.60 ± 0.30
N_{comptt}	$0.36^{+0.15}_{-0.22}$	$1.044^{+0.056}_{-0.059}$	0.710 ± 0.040
Flux _{comptt}	1.12	1.60	1.24
R_W (km)	20.5 ± 2.7	20.4 ± 1.4	19.0 ± 3.0
Photon Index	2.49 (fixed)	2.49 (fixed)	$2.49^{+0.15}_{-0.20}$
N_{po}	< 0.094	0.185 ± 0.036	$0.36^{+0.27}_{-0.20}$
Flux _{po}	< 0.09	0.18	0.36
$E_{\text{Fe XXV}}$ (keV)	$6.774^{+0.050}_{-0.053}$	$6.839^{+0.077}_{-0.083}$	6.740 ± 0.060
$\sigma_{\text{Fe XXV}}$ (keV)	$0.178^{+0.082}_{-0.097}$	< 0.22	0.24 ± 0.10
$I_{\text{Fe XXV}}$ ($\times 10^{-3}$)	$4.10^{+0.93}_{-0.79}$	$2.42^{+0.87}_{-0.67}$	$4.7^{+1.2}_{-0.9}$
L_{tot} ($\times 10^{38}$ erg s $^{-1}$)	1.3	1.7	1.4
E_{edge} (keV)	–	$9.06^{+0.29}_{-0.26}$	$9.24^{+0.19}_{-0.24}$
τ_{edge}	–	0.020 ± 0.010	0.043 ± 0.011
χ^2 (d.o.f.)	190 (174)	144 (176)	255 (198)

factor at all energies¹. To account for calibration uncertainties a systematic error of 1% was added to the data. As customary, in the spectral fitting procedure we allowed for a different normalization of the LECS, HPGSPC, and PDS spectra relative to the MECS spectrum, and we checked that the values obtained in the fits were in the standard range for each instrument. The energy ranges used for the spectral analysis were 0.12–1.5 keV for the LECS, 1–10 keV for the MECS, 8–30 keV for the HPGSPC, and 15–200 keV for the PDS. We indicated the three spectra corresponding to the intervals A, B, and C selected in the CD (see Fig. 2).

We fitted the continuum emission using the model applied by Lavagetto et al. (2004) to the spectrum C when GX 340+0 was probably in the HB. The model was composed of a blackbody plus the Comptonization model *Comptt* (Titarchuk, 1994) and an emission line at 6.8 keV, including the photoelectric absorption by neutral matter. In Table 3 we report the best parameters obtained from the fits of spectra A and B, and, for sake of clarity we report the results obtained by Lavagetto et al. (2004) for spectrum C (Observation 3).

We found that the best parameters associated to the blackbody do not change along the track of the source on the CD. We inferred a blackbody radius of 70 km suggesting that the corresponding emission originates away from the neutron star surface, probably in the inner radius of the accretion disk. The seed-photon temperature of the Comptonized component in spectra A and B (NB and NB/FB apex) is 1.1–1.2 keV, slightly larger than 0.9 keV obtained from spectrum C (HB). This could be explained assuming that the seed photons are produced on the neutron star surface, where the temperature increases because of the accretion rate increases going from the HB to the lower NB (see Fig. 2). The electron temperature is between 4 and 10 keV in the lower NB while it is 3 keV in the HB and upper NB. The optical depth associated to the Comptonized region decreases going from 13 at the HB to 3 at the NB/FB apex. Assuming a spherical geometry for the Comptonizing region we inferred that the seed photons came from 20 km, near the neutron star surface. The photon index of the power law was kept fixed in spectra A and B at 2.49, obtained from spectrum C. We note that the flux associated to this component decreases going from the HB to the FB. This behaviour is similar to those observed in other Z source as GX 17+2 (Di Salvo et al., 2000), and indicates that the increase of the accretion rate inhibits the formation of the power-law component at high energies. The Gaussian emission line associated to Fe XXV do not change in the three spectra.

Finally we note that the optical depth associated to the absorption edge at 9.2 keV seems to follow the behaviour of the Comptonized component decreasing from the HB to the NB/FB apex. This suggests that the absorption edge associated to Fe XXV could be produced in the same region near the neutron star.

Acknowledgements This work was partially supported by the Italian Space Agency (ASI) and the Ministero della Istruzione, della Università e della Ricerca (MIUR).

References

- Boella G., Butler R. C., Perola G. C., et al., 1997, *A&A*, 122, 299
 di Salvo, T., Stella L., Robba N. R., et al., 2000, *ApJ*, 544, L119
 Fender, R. P., & Hendry, M. A., 2000, *MNRAS*, 317, 1
 Friedman, H., Byram E. T., and Chubb, T. A., 1967, *Science*, 156, 374
 Hasinger, G., van der Klis, M., 1989, *A&A*, 225, 79
 Lavagetto, G., Iaria, R., di Salvo, T., et al., 2004, *Nuclear Physics B Proc. Supplements*, 132, 616
 Margon, B., Bowyer, S., Lampton, M., Cruddace, R., 1971, *ApJ*, 169, L45
 Miller, B. W., Margon, B., Burton, M. G., 1993, *AJ*, 106, 404
 Penninx, W., Zwarthoed, G. A. A., van Paradijs, J., et al., 1993, *A&A*, 267, 92
 Ponman, T., 1982, *MNRAS*, 201, 769
 Rappaport, S., Zaumen, W., Doxsey, R., Mayer, W., 1971, *ApJ*, 169, L93
 Schulz, N. S., Hasinger, G., Truemper, J., 1989, *A&A*, 225, 48
 Schulz, N. S., Wijers, R. A. M. J., 1993, *A&A*, 273, 123
 Titarchuk L., 1994, *ApJ*, 434, 570
 van Paradijs, J., Hasinger, G., Lewin, W. H. G., et al., 1988, *MNRAS*, 231, 379

¹ see the BeppoSAX cookbook at <http://www.sdc.asi.it/software/index.html>